Outdoor measurements of spherical acoustic shock decay

Sarah M. Young
Department of Physics, Brigham Young University–Idaho, Rexburg, Idaho 83460, USA
sarahmyoung24@gmail.com

Kent L. Gee, Tracianne B. Neilsen, and Kevin M. Leete
Department of Physics and Astronomy, Brigham Young University, Provo,
Utah 84602, USA
kentgee@byu.edu, tbn@byu.edu, kevinmatthewleete@gmail.com

Abstract: Prior anechoic measurements of a small acetylene-oxygen balloon explosion were used to study spherical weak-shock decay over short ranges [Muhlestein *et al.*, J. Acoust. Soc. Am. **131**, 2422–2430 (2012)]. Here, longer-range measurements conducted at the Bonneville Salt Flats with a larger balloon are described. Waveform and spectral characteristics and comparisons of the peak pressure decay with an analytical weak-shock model are presented. Weak shocks persist to at least 305 m, with an amplitude decay that is predicted reasonably well using the model. Deviations are discussed in the context of atmospheric effects and nonlinear ground reflections.
© 2015 Acoustical Society of America
[MH]

1. Introduction

Previous work by Muhlestein *et al.*[1] on short-range spherical acoustic shock propagation from small oxyacetelyne balloons motivated this Letter regarding outdoor measurements of larger-amplitude shock waves over greater distances. Their pedagogical example favorably compared anechoic measurements with an analytical model[2] for the spherical evolution of an ideal weak shock with exponentially decaying tail. The experiment described in this Letter uses a larger balloon in an outdoor setting, which results in a greater shock amplitude and propagation range but includes complications of ground reflections and meteorology as well.

In addition to historical work, summarized in monographs,[3,4] that led to scaling laws[5] for large chemical and nuclear explosions, the decay of spherical shocks have been described in various contexts. These include underwater explosions,[6] N-wave spark sources,[7] Gatling-gun muzzle blasts,[8] and plastic explosives,[9,10] the latter including measurements over different surfaces.[9] Related work on cylindrical ballistic shocks has also been performed.[11,12]

The present Letter describes gaseous, explosion-based shock evolution over a greater propagation range than other studies, such that the peak level decays nearly 80 dB. Additionally, it emphasizes the behavior and extent of the weak-shock regime as far as it relates to shock overpressure decay. Both the measurement location and time of day result in a relatively clean measurement whose waveforms, one-third octave sound exposure level (SEL), and peak sound pressure level (L_{pk}) decay can be studied in detail. The influence of ground reflections, atmospheric losses, and likely refraction are described.

2. Experimental description

The measurements were conducted on Utah's Bonneville Salt Flats, where the relatively flat ($\sim \pm 0.5$ cm variation in salt height), hard, and homogenous surface provides a simpler long-range propagation scenario than in the vast majority of outdoor studies. Not surprisingly, ground reflection measurements confirmed that the flats can be treated as acoustically hard, with an effective flow resistivity exceeding 5000 kPa s/m^2. The explosion data were collected between 6:00 and 10:00 am MDT when wind speeds are typically low. During the measurement window, the temperature increased from 23 to 31 °C with a decrease in relative humidity from 28% to 19%. During the measurement reported here, the ambient pressure, temperature, and relative humidity were 87 kPa, 29.0 °C, and 21%. A two-point temperature measurement indicated a slight inversion with an approximate gradient of 0.2 °C/m at a height of 1 m above the ground. The wind speed near balloon height was 3 m/s in a direction nearly

perpendicular to the measurement array. The ambient sound speed was calculated to be 348 ±1 m/s.

Spherical latex balloons were filled[1,13] with a stoichiometric ratio of oxygen and acetylene and taped to a tripod-mounted metal cradle at a height of 3.7 m (12 ft). A 56-cm diameter balloon (16 times the volume of the balloon in Ref. 1), was used for the test described here. A modified model rocket ignition system was used for detonation: the igniter was taped to the balloon base and the triggering distance was increased to 46 m for safety.

Acoustic pressure waveforms were acquired along a line from 0.9 m (3.0 ft) to 805 m (0.50 mi), as shown in Fig. 1. As with previous balloon,[1,14] military jet,[15] and rocket noise[16] measurements, data were recorded using National Instruments PXI-4462 dynamic signal acquisition devices, with the exception of the 805 m data, which were recorded using a USB-9233 sampling at 50 kHz. The PXI-4462 data were recorded at the maximum sampling rate, 204.8 kHz. PCB® piezoresistive pressure gages, three of which had an aluminum pencil-style housing intended specifically for blast noise measurements, were used for the closest measurements. Beyond 2 m, GRAS 6.35 mm 46BG, 40BD, and 40BE microphones were used without grid caps and oriented either skyward or toward the source according to microphone type. The 46BG and some 40BD microphones were designed with especially low sensitivies for near-field rocket noise measurements.[16] Because prior balloon measurements indicated approximate axisymmetry, acoustically speaking, the closest tripods were arranged at various angles to reduce the impact of scattering on the measured waveforms. Also to reduce scattering, the microphones were taped to the ends of dowels attached to the tripods. Excepting 805 m, every tripod had a microphone located at a height of 3.7 m (balloon height), with other microphone heights ranging from 0.30 to 6.1 m (1.0–20 ft).

3. Results and analysis

Three analyses are used to characterize the blast wave propagation. Pressure waveforms and SEL spectra at several distances are first examined. Afterward, the range-dependent decay in peak sound pressure, L_{pk}, is compared to that of an ideal weak shock with exponential tail, similar to Refs. 1, 6, and 8 though over a greater range of levels. Although a single explosion is analyzed in this Letter, similar trends were found from preliminary analysis of other balloon explosions. The blast waveforms at a height of 3.7 m (12.0 ft) are shown in Fig. 2 over a 10 ms window (2 ms per division) for several distances. In each panel, the approximate free-field shock overpressure, p_{sh}, is indicated by the dashed red line. For example, at $r = 0.9$ m, $p_{sh} = 152$ kPa, which is equivalent to $L_{pk} = 198$ dB re 20 μPa, when rounded to the nearest decibel. Because of Gibbs-like ringing[1] in the vicinity of the shock, due to both the data acquisition system and imperfect microphone orientation, the peak pressure was estimated by considering the slope immediately after the initial shock. The estimated uncertainty in peak pressure determination is ±1 dB.

Because of the shock's supersonic propagation, the waveform positive phase duration rapidly broadens, especially between 0.9 and 76 m. (Based on the peak pressure and ambient conditions, the calculated shock velocity at 0.9 m is 609 m/s.) At 76 m, the time scale remains more consistent because the shock velocity is within 1 m/s
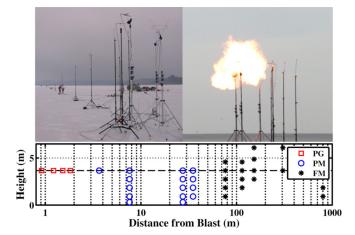

Fig. 1. (Color online) View of the microphone array on the Bonneville Salt Flats, a balloon explosion, and a schematic of piezoresistive gage (PG), pressure microphone (PM), and free-field microphone (FM) locations.
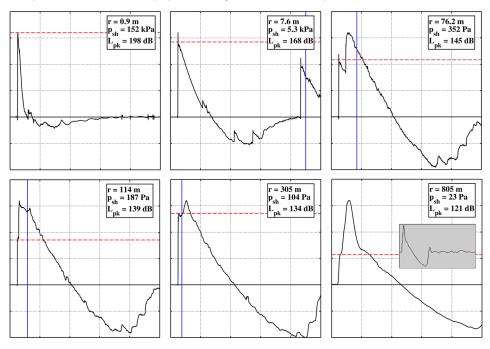
Fig. 2. (Color online) Blast waveforms over a 10 ms window for a 56 cm diameter oxyacetylene balloon explosion at ranges of 0.9, 7.6, 76.2, 114, 305, and 805 m and a height of 3.66 m. The dashed red line shows the peak pressure determined for the incident wave, while the blue line shows the predicted arrival of the ground reflection.

of the ambient sound speed. The characteristics of a rigid ground plane reflection are seen within the 10 ms window starting at 7.6 m. At 76 m, the ground-reflected shock wave has a rounder peak, probably due to surface roughness and near-ground microclimate. As range increases, the path length between direct and reflected paths lessens; at 114 m, the direct and reflected shocks nearly overlap. At 305 m, the incident wave is indistinguishable from the ground reflection, although there is a second, broader peak that occurs approximately 0.7 ms after the initial shock arrival.

The near merging of the direct and reflected shocks by 114 m is initially surprising but can be qualitatively explained via principles of Mach stem formation. The plots for the waveforms at 7.6, 76, 114, and 305 m show a blue vertical line corresponding to the expected time delay of the reflected shock relative to the direct shock arrival assuming a constant ambient sound speed. In each case, the reflected shock arrives earlier than expected. Although both shocks travel supersonically, which slightly changes the time delay, the relative arrival times cannot be reconciled without allowing that the ground-reflected shock travels *faster* than the incident shock. The greater shock velocity can be explained by the fact that the reflecting shock travels in the wake of the free-field shock wave, which elevates the air temperature. This decreases the time delay between the two shocks relative to the blue line. At 305 m, there is no apparent time delay in Fig. 2, which indicates a merging of the direct and reflected waves consistent with Mach stem formation.[17] This is also the case at 152 m, which is not shown. For our purposes, the creation of a Mach stem in the far field appears to approximately double the peak pressure; further analysis is beyond the scope of this Letter.

Although a 204.8 kHz sampling rate is insufficient to study rise-time characteristics in detail, the observed shock rise-time evolution is instructive. Inspection of the waveforms reveals that the initial shock rise time is two samples long (consisting of three data points), or approximately 10 μs for all the distances shown, as per the limits of 6.35 mm pressure microphones,[18] except at 305 and 805 m, which have rise times of approximately 15 and 140 μs, respectively. In other words, the shocks are considered near-ideal weak shocks within the sampling resolution and use of 6.35 mm microphones, but eventually begin to thicken because of atmospheric absorption.[10,11] The 805 m waveform's initial rise has the familiar hyperbolic tangent-like slope of a shock thickened due to losses. Determination of the 805 m peak pressure and rise time is complicated by the large, broad peak that occurs approximately 0.8 ms after the initial, thickened shock. However, the slight separation between the initial rise and the secondary peak allow estimation of the peak pressure, again to within approximately 1 dB.

The cause, and increasing significance with distance, of secondary peaks at 305 and 805 m is uncertain, but the arrival timing suggests an appreciably larger path length difference than exists in the measurement geometry. Furthermore, the fact that the secondary peak is not shock-like at 305 m and is relatively low-amplitude suggests a meteorology-related phenomenon. Our near-ground temperature measurements suggested a downward refracting atmosphere, with the possibility of rays reaching the microphone at later times through curved rays and possible ground bounces.[19] The atmosphere-induced multipath effect explanation is strengthened by the insert in the 805 m plot, which shows the waveform over a longer time scale. An additional positive peak at the waveform tail not present at closer distances is reminiscent of peaked sonic boom signatures[20] that deviate from classic N-wave behavior because of atmospheric effects, as well as additional "ringing" indicating late arrivals via other paths.

The conclusions made from the waveforms in Fig. 2 are strengthened by considering the one-third octave SEL, shown for several distances in Fig. 3. The supersonic shock propagation and resultant waveform stretching cause the peak frequency to decrease by more than an order of magnitude as distance increases. Second, a 10 dB/decade roll-off, indicative of weak-shock behavior, is maintained out to 40 kHz to at least 152 m. The high-frequency roll-off at 305 m appears to be ~12 dB/decade, which corresponds to the shock rise time beginning to increase. At 805 m, the spectral slope rolls off below 1 kHz, with generally more complicated behavior due to the high-amplitude secondary arrival. The ground reflections are also evident in the SEL. For the 0.9 and 1.2 m locations, the ground-reflected wave arrives with a sufficiently low amplitude and with a relatively large time delay that the interference nulls are not visible with the one-third octave integration. Beginning with the 7.6 m and continuing through the 114 m spectra, interference minima and maxima appear at increasingly higher frequencies, as the path length difference decreases. This behavior ceases at 152 m when the two waves have fully merged, creating one continuous wavefront with no significant ground interference null (cf. the 114 m SEL spectrum). For 114 m and beyond, there is an additional set of nulls beginning with the 125–160 Hz one-third octave bands that are more prominent with distance; these appear to be related to the secondary arrivals in the waveforms.

The SEL spectra reinforce the propagation characteristics observed in the waveform comparisons, with shock-like behavior persisting out to 305 m and other trends explained by the ground interaction and atmospheric influences. This permits meaningful comparisons of L_{pk} decay with the analytical weak-shock model used in the laboratory experiments[1] that preceded the present study. As input parameters, the model only requires knowledge of p_{sh} and the time required for the amplitude to decay to p_{sh}/e at a certain distance from the source. Initial application of the model suggested that perhaps the 0.9 m distance underestimated the true pressure because of the likelihood the probe was inside the blast itself. Thus, the modeled 0.9 m peak amplitude was increased by 3 dB such that the model fits both the 0.9 and 1.2 m data points, referred to as fit 1. Fit 2 uses the measured 1.5 m waveform parameters as input.
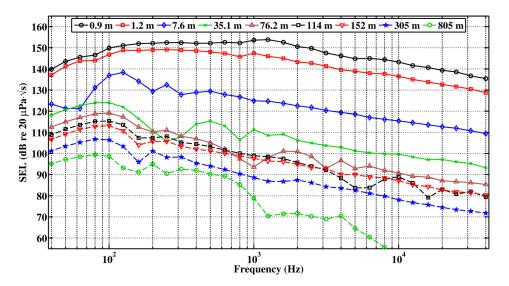

Fig. 3. (Color online) One-third octave band sound exposure level (SEL) for a 56 cm diameter oxyacetylene balloon.
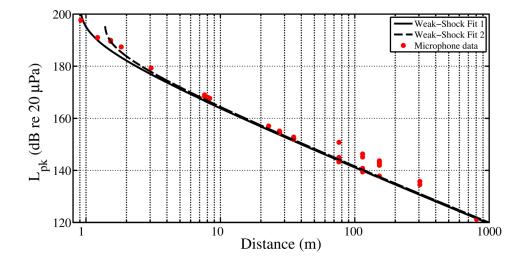
Fig. 4. (Color online) Peak sound level decay from a 56 cm diameter oxyacetylene balloon, along with two analytical weak-shock theory curves, based on an adjustment of the peak pressure at 0.9 m (fit 1) and using the parameters extracted directly from the 1.5 m waveform (fit 2).

The comparison of fits 1 and 2 with the L_{pk} estimated from the measured data is shown as a function of range in Fig. 4. Note that choice of input parameters results in very different behavior near the explosion, likely because of the finite-volume source and the fact that the peak levels exceed weak shock theory limits,[1,21] but in the far field, yield nearly identical results. Both analytical curves transition from a more rapid decay near the source into a 22.0 dB/decade roll-off after 30 m, which corresponds to the $r^{-1.1}$ far-field decay for p_{sh} described for nuclear and chemical explosions in ANSI S2.20–1983.[5] The analytical result closely follows the weak-shock theory decays of $r^{-1.13}$ of Rogers[6] and $r^{-1.14}$ by Wright.[7] In addition to the 3.7 m-high microphones, whose results are described in Figs. 2 and 3, the L_{pk} at other heights are also shown in Fig. 4. At 76 m, one of four microphones, located at a height of 0.30 m, has an approximate 6 dB level increase. At 114 m, the 0.30 and 0.61 m microphones see a similar increase. At 152 m, the three microphones 4.9 m and below have an increase, whereas the microphone at 6.1 m follows the free-field decay curve established near the source. By 305 m, the 3.7 and 6.1 m microphones both yield levels that are 4–5 dB above the weak-shock theory curve. At 805 m, the estimated peak level is just below the free-field weak-shock theory curve. Thus, between 76 and 805 m, the data suggest the formation of a merged wavefront (Mach stem) that grows in height with distance, essentially following the weak-shock decay rate but at an increased amplitude, before the shock front begins to thicken somewhere around 305 m and the L_{pk} decay rate increases. The close agreement at 805 m, despite the fact that the wave is no longer a weak shock, is the result of direct and ground reflected waves having merged during propagation.

4. Concluding discussion

This Letter has extended the scope of prior measurements involving spherically decaying shocks and an explicit comparison with weak-shock theory. Despite the complexities of outdoor measurements, meaningful comparisons are made through waveform and spectral analysis, with the identification of nonlinear ground reflections and Mach stem formation, shock thickening, and additional atmospheric effects. A few additional comments are merited. First, the waveforms themselves look very shock-like at the explosion limits, which disagrees with Ref. 5 in its description of gaseous explosions as requiring significant distances to take on traditional propagation characteristics. It is true that the waveforms do not follow either weak-shock theory fit within the first few meters, but 3 m is less than six source diameters and a well-defined classical blast wave exists. Second, good agreement with the weak-shock model is seen at peak levels well beyond the traditional limits of weak-shock theory.[21] Third, the peak pressure decay curve shown is unique in the literature, in that free-field and Mach reflection data are separated and include the regime where linear losses are present. Analysis of blast noise data from larger and smaller balloons, including peak pressure decay, correlation with weather conditions, and the appearance of Mach stems will be useful in further examining the present conclusions.

Acknowledgments

References and links

[1] M. B. Muhlestein, K. L. Gee, and J. H. Macedone, "Educational demonstration of a spherically propagating acoustic shock," J. Acoust. Soc. Am. **131**, 2422–2430 (2012).

[2] D. T. Blackstock, "Propagation of a weak shock followed by a tail of arbitrary waveform," in *Proceedings of the 11th International Congress on Acoustics*, Paris, France (1983), Vol. 1, pp. 305–308.

[3] G. F. Kinney and K. J. Graham, *Explosive Shocks in Air* (Springer, Berlin, 1985), pp. 50–136.

[4] W. E. Baker, *Explosions in Air* (University of Texas Press, Austin, TX, 1973), pp. 1–77, 118–163.

[5] ANSI S2.20-1983: *American National Standard for Estimating Airblast Characteristics for Single Point Explosions in Air* (Acoustical Society of America, Melville, NY, 2006).

[6] P. Rogers, "Weak-shock solution for underwater explosive shock waves," J. Acoust. Soc. Am. **62**, 1412–1419 (1977).

[7] W. M. Wright, "Propagation in air of N waves produced by sparks," J. Acoust. Soc. Am. **73**, 1948–1955 (1983).

[8] M. D. Shaw and K. L. Gee, "Acoustical analysis of an indoor test facility for a 30-mm Gatling gun," Noise Control Eng. J. **58**, 611–620 (2010).

[9] R. D. Ford, D. J. Saunders, and G. Kerry, "The acoustic pressure waveform from small unconfined charges of plastic explosive," J. Acoust. Soc. Am. **94**, 408–417 (1993).

[10] A. Loubeau, V. W. Sparrow, L. L. Pater, and W. M. Wright, "High frequency measurements of blast wave propagation," J. Acoust. Soc. Am. **120**, EL29–EL35 (2006).

[11] H. E. Bass, B. A. Layton, L. N. Bolen, and R. Raspet, "Propagation of medium strength shock waves through the atmosphere," J. Acoust. Soc. Am. **82**, 306–310 (1987).

[12] R. Stoughton, "Measurements of small caliber ballistic shock waves in air," J. Acoust. Soc. Am. **102**, 781–787 (1997).

[13] K. L. Gee, J. A. Vernon, and J. H. Macedone, "Auditory risk of exploding hydrogen–oxygen balloons," J. Chem. Ed. **87**, 1039–1044 (2010).

[14] J. A. Vernon, K. L. Gee, and J. H. Macedone, "Acoustical characterization of exploding hydrogen-oxygen balloons," J. Acoust. Soc. Am. **131**, EL243–EL249 (2012).

[15] A. T. Wall, K. L. Gee, M. M. James, K. A. Bradley, S. A. McInerny, and T. B. Neilsen, "Near-field noise measurements of a high-performance military jet aircraft," Noise Control Eng. J. **60**, 421–434 (2012).

[16] K. L. Gee, J. H. Giraud, J. D. Blotter, and S. D. Sommerfeldt, "Near-field acoustic intensity measurements of a small solid rocket motor," J. Acoust. Soc. Am. **128**, EL69–EL74 (2010).

[17] G. Ben-Dor, *Shock Wave Reflection Phenomena*, 2nd ed. (Springer, Berlin, 2007), pp. 1–38, 247–306.

[18] T. B. Gabrielson, T. M. Marston, and A. A. Atchley, "Nonlinear propagation modeling: Guidelines for supporting measurements," Proc. Noise-Con **114**, 275–285 (2005).

[19] D. K. Wilson, "The sound-speed gradient and refraction in the near ground atmosphere," J. Acoust. Soc. Am. **113**, 750–757 (2003).

[20] D. J. Maglieri and K. J. Plotkin, "Sonic Boom," in *Noise Sources,* Vol. 1 of *Aeroacoustics of Flight Vehicles: Theory and Practice*, edited by H. H. Hubbard (Acoustical Society of America, Woodbury, NY, 1995), Chap. 10, pp. 523–525.

[21] F. M. Pestorius and S. B. Williams, "Upper limit on the use of weak-shock theory," J. Acoust. Soc. Am. **55**, 1334–1335 (1974).